Mon. Not. R. Astron. Soc. **327,** 1273–1278 (2001)

A relativistic jet from Cygnus X-1 in the low/hard X-ray state

A. M. Stirling,[1,2] R. E. Spencer,[2] C. J. de la Force,[2] M. A. Garrett,[3] R. P. Fender[4] and R. N. Ogley[5]

[1]*CFA, University of Central Lancashire, Preston PR1 2HE*
[2]*University of Manchester, Jodrell Bank Observatory, Macclesfield, Cheshire SK11 9DL*
[3]*Joint Institute for VLBI in Europe, Postbus 2, 7990 AA Dwingeloo, the Netherlands*
[4]*Astronomical Institute 'Anton Pannekoek' and Centre for High–Energy Astrophysics, University of Amsterdam, Kruislaan 403, 1098 SJ Amsterdam, the Netherlands*
[5]*Physics Department, Keele University, Staffordshire ST5 5BG*

Accepted 2001 July 10. Received 2001 June 18; in original form 2000 December 11

ABSTRACT

We present the detection of a radio-emitting jet from the black hole candidate and X-ray binary source Cygnus X-1. Evidence of a bright core with a slightly extended structure was found on milliarcsecond resolution observations with the Very Long Baseline Array (VLBA) at 15.4 GHz. Later observations with the VLBA [and including the phased-up, Very Large Array (VLA)] at 8.4 GHz show an extended jet-like feature extending to ~ 15 mas from a core region, with an opening angle of $< 2°$. In addition, lower resolution MERLIN observations at 5 GHz show that the source has < 10 per cent linear polarization. The source was in the low/hard X-ray state during the observations, and the results confirm the existence of persistent radio emission from an unresolved core and a variable, relativistic ($> 0.6c$) jet during this state.

Key words: binaries: close – stars: individual: Cygnus X-1 – ISM: jets and outflows.

1 INTRODUCTION

Of the ~ 250 currently known X-ray binaries, approximately 50 have detectable radio emission and a dozen or so of these have been found to have radio jets. Extreme examples of the jet sources are GRS 1915+105 (Mirabel & Rodriguez 1994; Fender et al. 1999a) and GRO J1655–40 (Hjellming & Rupen 1995; Tingay et al. 1995), both exhibiting apparent superluminal motion. Such jet sources often show strong radio flux variability (see Fender, Burnell & Waltman 1997 for a review). However, some sources show relatively little variation, such as Cygnus X-1 and LS 5039. The persistently radio-emitting (20–40 mJy) LS 5039, which is at a similar distance, has been shown to have a milliarcsecond-scale jet (Parades et al. 2000).

Cygnus X-1 (HDE 226868, V1357 Cygni) comprises a supergiant secondary (spectral type O9.7 Iab) with mass between 20–33 $M_\odot$ together with a compact primary which is a strong black hole candidate with mass between 7 and 16 $M_\odot$. The orbital period has been detected in optical, UV, X-ray and radio wavelengths (Pooley, Fender & Brocksopp 1999; Brocksopp et al. 1999b). The orbital period is ~ 5.6 d and an orbital radius of 0.2 au is derived; at an assumed distance of 2 kpc (Gierliński et al. 1999) this corresponds to an angular scale of 0.1 milliarcsec (mas). An orbital ephemeris has been derived from optical radial velocity data (LaSala et al. 1998) and compared with other wavelength data (Brocksopp et al. 1999b).

The source has been fairly stable in the low/hard X-ray state, at around 15 mJy at cm wavelengths and with an extremely flat radio spectrum. The radio emission was first observed following a 'turn on' corresponding to a X-ray state change in 1972. The 'turn on' was probably the recovery from a high/soft state during which time the jet had been quenched, as Zhang et al. (1997) show that the radio emission was similarly suppressed during the high/soft X-ray state in 1996. This is behaviour similar to that shown by GX 339–4 during 1998 (Fender et al. 1999b).

At 15 GHz, a quasi-sinusoidal 3-mJy semi-amplitude modulation is observed superimposed on the 14-mJy mean level. The minimum occurs at superior conjunction of the compact body, implying that the radio-emitting region is associated with this compact object (Pooley et al. 1999). More recently a further modulation period of 142 d has been detected (Brocksopp et al. 1999b), explained as precession or warping of the disc. The source displays a flat spectrum between 2 and 220 GHz, with an average spectral index $|\alpha| \leq 0.15$ (Fender et al. 2000). A small radio flare coincident with an X-ray flare in 1975 further demonstrated an X-ray/radio correlation (Hjellming & Han 1995). Both the observed flat spectrum and the orbital modulation fit into the slowed adiabatically expanding conical radio jet model (Hjellming & Johnston 1988). It is not clear how common the small flares (less than ~ 30 mJy) are or exactly how the X-ray state changes affect the radio emission (Brocksopp et al. 1999b).

An accretion disc is essential in models of the X-ray variability.

The source has high/soft, low/hard and intermediate spectral states, spending most time in the low/hard X-ray state. The X-ray state changes can be modelled using a variable accretion rate; when the accretion rate is low an advection-dominated accretion flow (ADAF) is postulated (Esin et al. 1998), giving a low radiative efficiency, as expected for such underluminous quiescent sources. The existence of a jet perpendicular to the disc implies that the outflow process may be important in terms of mass and angular momentum loss from the disc.

Previous radio maps on both Very Large Array (VLA) (Marti et al. 1996) and MERLIN (Newell 1997) size scales [5 arcsec and 50 mas beam full width at half maximum (FWHM) respectively] showed no conclusive evidence for resolved or extended emission. The VLA image showed emission regions to the north and south which could be lobes associated with the source at an extent of ~ 5 arcmin.

2 VLBI AND MERLIN OBSERVATIONS

For over a decade Cygnus X-1 has been employed as an astrometric reference source (Lestrade et al. 1995). Variations in the visibility amplitude were observed on the very longest transatlantic baselines (Lestrade, private communication), suggesting resolved source structure on the milliarcsec scale. To investigate the milliarcsec source structure in more detail, we obtained full track, 15.4-GHz Very Long Baseline Array (VLBA) observations of the source in 1997. These were subsequently followed up in 1998 with multi-epoch and multi-frequency 8.4- and 15.4-GHz observations. The initial 15.4-GHz observations and the later 8.4-GHz multi-epoch observations are discussed in this paper. The multi-epoch 15.4-GHz observations will be presented in a separate paper (de La Force et al., in preparation). In this paper we also present the results of an analysis of archive MERLIN data, investigating the linear polarization properties of Cygnus X-1.

2.1 Initial 15.4-GHz VLBA observations

On 1997 March 28 the VLBA interferometer network was used to observe a single epoch of Cygnus X-1 at 15.4 GHz while the source was in the low/hard X-ray state. The run was made at 10 : 15–19 : 45 UT (centred on Julian date 245 0901.06), recording at a sustained rate of 128 Mbits per second. Only one hand of polarization was recorded in left-hand circular polarization (LCP), providing a total bandwidth of 64 MHz. The observations were made in phase-reference mode with a typical cycle time of 2.0 min on the phase-calibrator and 2.0 min on the target, Cygnus X-1. The phase-calibrator used throughout these observations was B1955+335, a bright ($S_{15\,\mathrm{GHz}} \sim 300$ mJy), compact radio source (with an accurately measured astrometric International Celestial Reference Frame position) lying within 1.°1 of Cygnus X-1. The data were correlated at the NRAO correlator in Socorro, New Mexico, USA. The coordinates chosen to correlate the data were those given by the most recent published radio position, $19^{\mathrm{h}}58^{\mathrm{m}}21\overset{\mathrm{s}}{.}680$ $+35°12'05\overset{''}{.}887$ (epoch 1986, J2000) Lestrade et al. (1995). With a total of 8 h observing time excellent *uv* coverage of the target source was obtained.

The initial analysis of the data was performed with the NRAO AIPS package (e.g. Fomalont 1981). The visibility amplitudes were calibrated using the system temperatures and gain information provided by each of the telescopes. Occasional observations of 3C 345 were used to align the individual 8-MHz sub-bands (IFs) that spanned the total 64-MHz bandwidth. The antenna residual delays, fringe rates and gain corrections were determined from the phase calibrator and interpolated and applied to the target, Cygnus X-1.

Unfortunately, the positions we supplied to the correlator did not take into account the proper motion of Cygnus X-1. Thus our first map made from the calibrated Cygnus X-1 data showed no radio emission in the centre of the map but obvious side-lobe structure from a source apparently located outside the field was clearly visible. A wide field image of the region (for which no averaging of the data were performed) revealed this source to be Cygnus X-1, offset 46 mas to the east and 84 mas to the south of the nominal phase-centre. Our position, after correcting for the measured proper motion of the source (provided by Lestrade, private communication) is within 1.5 mas of the original astrometric position (Lestrade et al. 1995). The refined proper motion is 8.7 ± 0.2 mas yr^{-1} in position angle (PA) $-151 \pm 1°$.

The Cygnus X-1 data were Fourier transformed and then CLEANed using the AIPS task IMAGR, which allows variable data weighting using the robust parameter (Briggs 1995). No self-calibration of the data was performed. A naturally weighted (robust 5) image is presented in Fig. 1. The elliptical Gaussian restoring beam measures 1.13×0.63 mas^2 in PA 12.°9.

The source is clearly detected, and is plotted relative to the epoch 1986 coordinates chosen for correlation. The structure is confused and ambiguous; this is likely due to errors in the phase referencing process. Unfortunately the source was too weak for reliable self-calibration with this observing array. An attempt to model fit these data as a single component with DIFMAP (Pearson et al. 1994) suggested an extension in PA $-15° \pm 5°$ (Stirling, Spencer & Garrett 1998). It seems likely that the radio emission represents an unresolved radio jet.

2.2 Follow-up VLBA multi-epoch 8.4-GHz observations

2.2.1 *Observations and data reduction*

Further high-resolution observations of Cygnus X-1 were made in 1998 August with the VLBA and VLA. Three epochs of observations were obtained every 2 d to cover a large fraction of

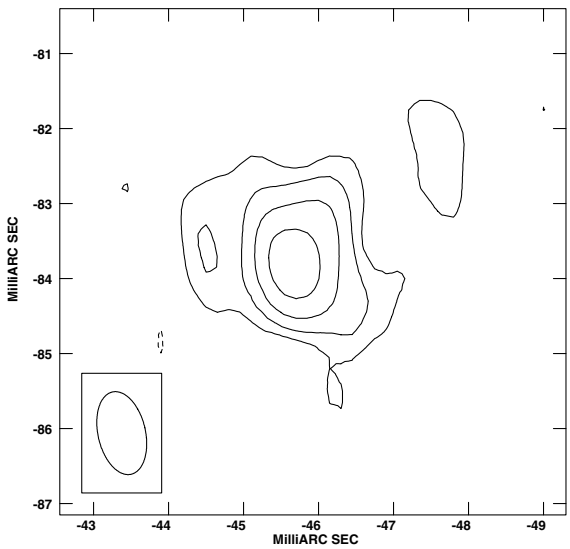

Figure 1. The naturally weighted VLBA image of Cygnus X-1 from 1997 March 28 at 15.4 GHz has a lowest contour of 0.4 mJy beam^{-1} and a peak flux density of 5.0 mJy beam^{-1}. As with all images in this paper, the contouring represents factors of 2.

the period (5.6 d) of the binary system. The runs were made at 04 : 19–08 : 55 UT on the 10th, (epoch A) at 04 : 20–08 : 30 UT on the 12th (epoch B) and at 04 : 20–08 : 30 UT on the 14th (epoch C). The mid-point of each observation was on Julian date 245 1035.76 (A), 245 1037.76 (B) and 245 1039.76 (C). Observations were made at 15.4 and 8.4 GHz, the frequencies being alternated each hour. Only the 8.4-GHz data are considered in this paper.

As the source is relatively weak, the phased VLA was also included as one element in the array. A data rate of 256 Mbits per second was used (recording LCP in 8×8 MHz sub-bands, 2-bit sampled at the Nyquist rate). The Cygnus X-1 data were correlated using a position of $19^{\rm h}58^{\rm m}21\overset{\rm s}{.}67634$ $+35°12'05\overset{''}{.}7940$, J2000 (derived from our earlier 15.4-GHz observations but with the source proper motion now included). The data analysis followed the standard procedure described earlier in Section 2.1.

2.2.2 *Images and component fluxes*

Owing to thunder storms and bad weather at the VLA, the third epoch had generally noisier data on the most sensitive VLA–VLBA baselines. The three naturally weighted images at 8.4 GHz have been self-calibrated in AIPS (using the extremely sensitive 'phased' VLA as a reference antenna) and are presented in Fig. 2 with identical contouring. Here the radio emission from a jet to the north-west is much clearer, extending out to ~ 15 mas from the core. The unresolved core likely represents the base of the visible jet and its flux density variations with orbital phase are given in Table 1.

There is some correlation between orbital ephemeris (from Brocksopp et al. 1999a) and the flux densities measured from our maps, as the unresolved core flux density has a maximum around inferior conjunction (see Table 1) and the orbital phase modulation of the radio flux does indeed imply that the radio flux variation should originate in or near the core, as observed. The flare preceding our observations by around 15 d as shown in Brocksopp et al. (1999b) may complicate the integrated flux density and period relationship found by Pooley et al. (1999).

2.3 MERLIN archival data

As all of the VLBA observations were made using a single hand of polarization, it was impossible to examine the linear polarization emitted from the jet. As MERLIN observes in all four polarization correlations as standard, linearly polarized emission can be imaged. Only the total intensity (Stokes *I*) image was presented by Newell (1997).

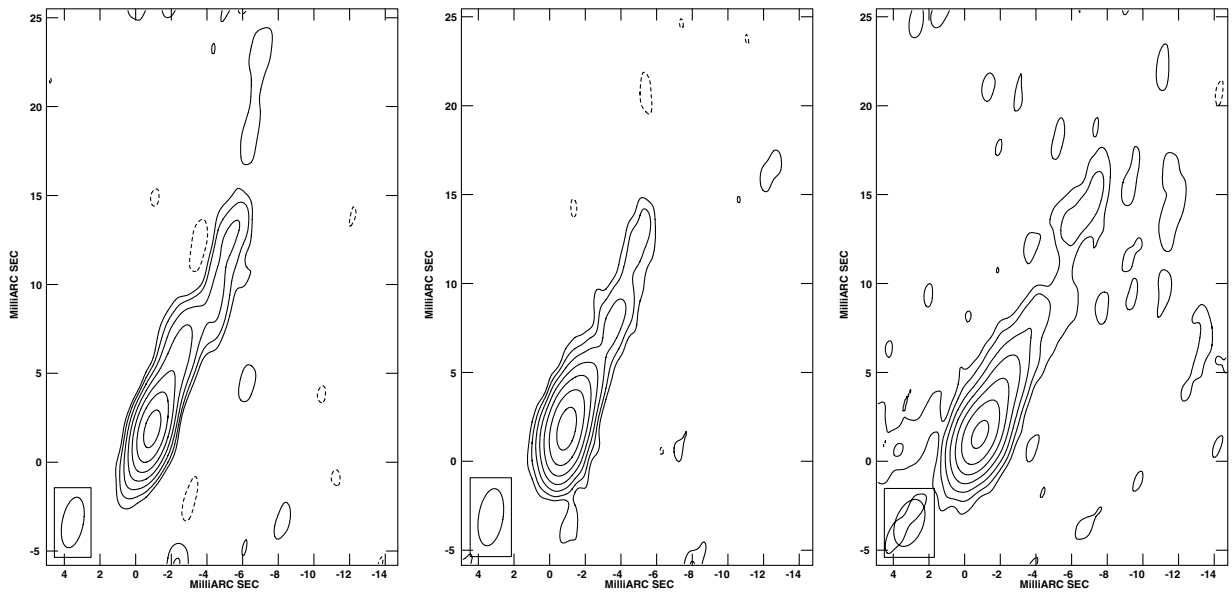

Figure 2. VLBA and phased VLA images of Cygnus X-1 from 1998 August, at 8 GHz; lowest contour 0.1 mJy. Epoch A is on the left with peak flux density 8.7 mJy beam^{-1} and convolved with a Gaussian beam 2.88×1.19 mas^2 in PA $-10\overset{\circ}{.}9$, epoch B in the middle with peak flux density 9.0 mJy beam^{-1} and convolved with a Gaussian beam 3.24×1.37 mas^2 in PA $-8\overset{\circ}{.}9$ and epoch C on the right with peak flux density 7.7 mJy beam^{-1} and convolved with a Gaussian beam 2.76×1.56 mas^2 in PA $-20\overset{\circ}{.}5$.

Table 1. Image properties for Cygnus X-1 at 8.4 GHz in August, 1998. Flux calibration is typically accurate to 5 per cent for VLBA images at this frequency. The unresolved flux densities per beam were derived from the uniformly weighted (robust −5) images, which are not presented in this paper.

Epoch (1998)	Orbital phase	Total flux density (mJy)	Unresolved core (mJy beam^{-1})	Jet (mJy)	Off source r.m.s. (mJy beam^{-1})
A	0.96	13.0	6.9	6.1	0.04
B	0.32	11.1	8.0	3.1	0.04
C	0.68	11.9	6.0	5.9	0.05

These MERLIN data, observed on 1995 July 19, were retrieved from the archives and calibrated in full polarization using the MERLIN pipeline (Thomasson et al. 1993). The 5-GHz observations were made in the standard MERLIN continuum setup over a bandwidth of 16 MHz. Also observed were a phase reference source, 1951+355; a flux and polarization PA calibrator, 3C286; and a point source calibrator, OQ208. The total intensity map of Cygnus X-1 was convolved with a Gaussian beam of $58 \times 37\,\mathrm{mas}^2$ in PA–81°.2 and found to be a point source with a peak flux density of $11.9 \pm 0.6\,\mathrm{mJy\,beam}^{-1}$, in agreement with Newell (1997). No linear polarization was detected associated with the source to an upper limit of $0.9\,\mathrm{mJy\,beam}^{-1}$, ruling out a simple, very ordered field structure.

3 ANALYSIS OF THESE AUGUST 1998 DATA

3.1 Emission mechanism

We can place a lower limit on the brightness temperature of the unresolved radio emission simply by using the Rayleigh–Jeans approximation. Using a flux density of 6 mJy and a solid angle equivalent to the uniform beam (epoch B) we derive a minimum temperature of 10^7 K at 8.4 GHz, inferring that the radiation is non-thermal, and is not for example caused by free–free emission from gas at 10^4 K. The observed spectral index and the detection of polarization in a number of jet sources suggest that the radiation is via the synchrotron mechanism. A spectral break is not observed in the radio or mm regimes, implying that the emitting electrons do not suffer significant radiative losses (Fender et al. 2000). The flat spectral index supports the non-thermal interpretation, and is often attributed to multiple expanding synchrotron-emitting regions within the beam when observed in the jets from quasars.

3.2 Doppler boosting

Following the method of Mirabel & Rodriguez (1994), under the assumption of an intrinsically symmetric ejection, then for bulk motions at a jet velocity β, the observed ratio of the approaching jet component, flux density, $S_{\rm app}$, to the receding jet components flux density, $S_{\rm rec}$, (assuming optically thin components or non-overlapping optically thick components), is given by

$$\frac{S_{\rm app}}{S_{\rm rec}} = \left(\frac{1+\beta\cos i}{1-\beta\cos i}\right)^{k-\alpha}, \qquad (1)$$

with $S_\nu \propto \nu^{+\alpha}$; $k = 2$ for a continuous jet and $k = 3$ for discrete plasmons; i is the angle to the line of sight. If the source is optically thick in places then the full radiation transfer equation must be solved, and then equation (1) gives only an approximation to β (Lind & Blandford 1985); see e.g. Cawthorne (1991) for a derivation of the (rather small) correction factors for a partially optically thick and continuous jet.

As we cannot measure the motion of individual components in both the receding and approaching jets, we cannot directly derive both β and i and hence the index $k - \alpha$. However we note that the average accretion disc axis, i, (and hence the jet) is likely to be around 40° to the line of sight (Bruevich et al. 1978), although this is not well defined (Brocksopp et al. 1999b). We use the angle to the line of sight to derive β for various values of $k - \alpha$.

We assume that we see only one side of the jet in our epoch A and use a ratio of approaching and receding flux densities of 50 to derive lower limits to the jet speed. The ratio is derived by assuming the receding jet flux is ≤ 6 beams $\times$ rms noise per beam, with 6 beams the extent of the approaching jet. Although the unresolved flux monitoring suggests a spectral index of around 0, using -0.6 gives a lower limit to β (it is unlikely that a synchrotron spectrum is much steeper than -0.6). We derive β for spectral indices of 0 and -0.6 and for both the continuous and discrete cases (Table 2). Errors from the poorly constrained angle to the line of sight dominate these calculations and the results should be regarded as order-of-magnitude only, especially as any possible attenuation of radiation from the receding jet by external free–free absorption cannot be quantified with a single frequency. The derived lower limits to β suggest the jet is at least moderately relativistic $> 0.6c$.

Table 2. Lower limits to the jet velocity as a fraction of c for various jet compositions.

Spectral index	Jet type	lower limit to β
0	continuous	0.97
0	discrete	0.74
−0.6	continuous	0.83
−0.6	discrete	0.63

The longer time-scale precessional period (142 d) of Cygnus X-1, where the deviation of the plane of the disc from the orbital plane, δ, may reach as much as $\sim 37°$ (Brocksopp et al. 1999b) is a further uncertainty. Soft X-ray monitoring (Brocksopp et al. 1999b) suggests that the soft X-ray intensity is mid-way between extrema during our observations; therefore the disc is close to its average inclination.

The emitted synchrotron intensity of the jet scales with the Doppler factor, D (e.g. Cawthorne 1991), to a power $\geq (2 - \alpha)$. For β of 0.75 and $i = 40°$ we find $D = 1.55$. Using the observed long-term variations in total flux of ≤ 3 mJy gives a maximum value for δ (assuming, say, $\alpha = 0$ for the radio jet) of only 4°. Therefore either the jet velocity is non-relativistic (and hence $D \sim 1$) or the actual precession of the jet is small compared with that suggested for the soft X-ray emitting region of the disc. Given our lower limits to β (in Table 2) we suggest that the inner part of the disc may be precessing at significantly less than the angle of around $\sim 37°$ suggested by soft X-ray monitoring. One solution to this would be a twisted accretion disc as postulated for SS433 (Sharp, Calvani &Turolla 1984). Alternatively the $\sim$ 142-d 'period' is a time scale for changes in the accretion rate, as is likely in GX 339–4 (Corbel et al. 2000). The extended emission on VLA scales (Marti et al. 1996) may be consistent with our measured jet position angle, particularly if the several mas per year south-west proper motion is considered.

3.3 A continuous and bending jet?

The higher resolution (robust 0 or partial uniform weighting) image in Fig. 3 was made using epoch A, the best set of 8.4-GHz data. Even with a resolving beam significantly smaller than that provided by natural weighting the jet still appears continuous in Fig. 3, although with small variations along it and a general decrease in brightness along the jet. Even at this resolution we may find that we are not resolving multiple discrete components (as was not discovered in SS433 until detailed VLBI observations were made).

Epoch A shows a pronounced bend or kink at around 7 mas from the radio core. The jet region at 8–15 mas subtends a similar

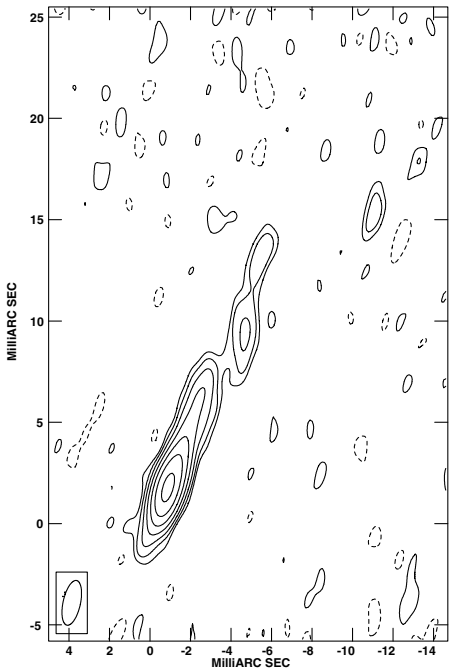

Figure 3. A high-resolution (robust 0) image of Cygnus X-1 at 8.4 GHz; lowest contour 0.157 mJy beam^{-1}, convolved with a Gaussian beam 2.25 × 0.86 mas^2 in PA −12°.4.

position angle from the core (21°–24°) in all 3 epochs, whereas the inner jet (< 7 mas) is at 17° during epoch A. The apparent change in direction of the jet suggests that the position angle of ejection is varying, perhaps either jet precession or jitter, both of which are observed in SS433 (Margon & Anderson 1989). It is also possible that the kinks observed in the extended emission are consistent with a bending jet flow, rather than a ballistic motion, although apparently unrelated to the direction of the proper motion of Cygnus X-1 as would be expected from ram pressure considerations. Projection effects will enhance the appearance of a jet bend (as with apparent 90° bends in blazar jets). The higher resolution image in Fig. 3 shows that the bend occurs in a minimum of surface brightness. This is consistent with an underlying helical magnetic field in which the magnetic field pitch angle reverses sign at the bend in radio structure, e.g. Laing (1981); Papageorgiou (private communication). Measurements of any linear polarization could confirm this model.

The bend is no longer apparent in epochs B and C, suggesting that the feature disappears on a time scale of ≤ 2 d. This could be due to rapid motion and decay via adiabatic expansion, or synchrotron losses. In the latter case the magnetic field in the component would need to be greater than 16 G, rather higher than is commonly deduced for microquasar jets.

It is also apparent in Fig. 3 that the jet is not resolved perpendicular to the flow. Using a beam size of 1 mas across the jet and a maximum distance from the core of 15 mas on the plane of the sky, the opening semi-angle of the radio-emitting material is constrained to ≤ 2°.

The flat radio spectrum in Cygnus X-1 has specifically been modelled as slowed expansion in a continuous jet (Hjellming & Johnston 1988). The predicted spectrum for this geometry is flat until a turnover at around 10 GHz for an inclination of 40°. However, the self-absorption in a slowed expanding jet model cannot explain the observed flat spectrum to mm wavelengths (Fender et al. 2000). In comparison, jet components from GRS 1915+105 are observed to become optically thin less than a few minutes after ejection at mm wavelengths (Mirabel et al. 1998). Possibly another inverted spectrum component (such as the disc or stellar wind), as well as the partially self-absorbed conical jet, is required to explain the wavelength dependence up to mm wavelengths of the integrated spectrum.

4 CONCLUSIONS

Cygnus X-1 has been detected with the VLBA at 15.4 GHz, giving a 13-year time base for proper motion measurements. Subsequent imaging at 8.4 GHz shows that a relativistic jet with either a bending flow or a variable ejection angle exists in Cygnus X-1. The jet appears to be narrow (< 2° opening angle). The source was known to be in a low/hard X-ray state at the times of all our observations. Given the documented X-ray/radio correlations, and our three separate images of extended radio emission, it is likely that a jet always exists in the 'quiescent' low/hard X-ray state thought to harbour a central ADAF. It is unclear how the low-level radio flaring of the low/hard X-ray state fits into the picture of a steady-state accretion disc input/output system.

Further VLBI observations with a global VLBI array were undertaken in 2001 May. A sequence of images within a day should show whether the radio jet is continuous or consists of moving discrete components.

ACKNOWLEDGMENTS

We thank Guy Pooley for flux monitoring efforts and J.-F. Lestrade for providing accurate proper motion data. Discussion with Tim Cawthorne, Denise Gabuzda and Zsolt Paragi improved the scope of this paper significantly. MERLIN is a national facility operated by the University of Manchester on behalf of PPARC. We thank Anita Richards for retrieval and initial calibration of the MERLIN archive data. The NRAO is operated by Associated Universities Inc. on behalf of the National Science Foundation. CJD and AMS acknowledge support from PPARC studentships during the bulk of this work. AMS is currently supported by a PPARC research grant.

REFERENCES

Briggs D. S., 1995, Am. Astron. Soc. Meeting, 187, 11202
Brocksopp C., Tarasov A. E., Lyuty V. M., Roche P., 1999a, A&A, 343, 861
Brocksopp C., Fender R. P., Larionov V., Lyuty V. M., Tarasov A. E., Pooley G. G., Paciesas W. S., Roche P., 1999b, MNRAS, 309, 1063
Bruevich V. V., Kilyachkov N. N., Sunyaev R. A., Shevchenko V. S., 1978, Pis'ma Astron Zh., 4, 544
Cawthorne T. V., 1991, Beams and Jets, Cambridge Astrophysics Series. Ch. 4 , p. 204
Corbel S., Fender R. P., Tzioumis A. K., Nowak M., McIntyre V., Durouchoux P., Sood R., 2000, A&A, 359, 251
Esin A. A., Narayan R., Cui W., Grove J. E., Zhang S., 1998, ApJ, 505, 854
Fender R. P., Burnell S. J. B., Waltman E. B., 1997, Vistas Astron, 41, 3
Fender R. P., Garrington S. T., McKay D. J., Pooley G. G., Spencer R. E., Stirling A. M., Waltmann E. B., 1999a, MNRAS, 304, 865
Fender R. P. et al., 1999b, ApJ, 519, L165
Fender R. P., Pooley G. G., Durouchoux P., Tilanus R. P. J., Brocksopp C., 2000, MNRAS, 312, 853
Fomalont E. B., 1981, News. NRAO, 3, 3
Gierliński M. G., Zdziarski A. A., Poutanen J., Coppi P. S., Ebisawa K., Johnson W. N., 1999, MNRAS, 309, 496
Hjellming R. M., Han X. H., 1995, X-ray Binaries, Cambridge Astrophysics Series. Ch. 7
Hjellming R. M., Johnston K. J., 1988, ApJ, 328, 600

Hjellming R. M., Rupen M. P., 1995, Nat, 375, 464
Laing R. A., 1981, ApJ, 248, 87
LaSala J., Charles P. A., Smith R. A. D., Balucinska-Church M., Church M. J., 1998, MNRAS, 301, 285
Lestrade J.-F. et al., 1995, A&A., 304, 182
Lind K. R., Blandford R. D., 1985, ApJ, 295, 358
Margon B., Anderson S. F., 1989, ApJ, 347, 448
Marti J., Rodriguez L. F., Mirabel I. F., Paredes J. M., A&A. 306, 4491996,
Mirabel I. F., Rodriguez L. F., 1994, Nat, 371, 46
Mirabel I. F., Dhawan V., Chaty S., Marti J., Robinson C. R., Swank J., Geballe T., 1998, A&A., 330, L9
Newell S. J., 1997, PhD thesis, Univ. Manchester
Paredes J. M., Marti J., Ribo M., Massi M., 2000, Sci, 288, 2340
Pearson T. J., Shepherd M. C., Taylor G. B., Myers S. T., 1994, Am. Astron. Soc. Meeting, 185, 808
Pooley G. G., Fender R. P., Brocksopp C., 1999, MNRAS, 302, L1
Sharp N. A., Calvani M., Turolla R., 1984, Comments Astrophys., 10, 53
Stirling A. M., Spencer R. E., Garrett M. A., 1998, New Astron. Rev., 42, 657
Thomasson P., Garrington S. T., Muxlow T. W. B., Leahy J. P., 1993, MERLIN user guide, Univ. of Manchester
Tingay S. J. et al., 1995, Nat, 374, 141
Zhang S. N., Mirabel I. F., Harmon B. A., Kroeger R. A., Rodriguez L. F., Hjellming R. M., Rupen M. P., 1997, in Dermer C. D., Strickman M. S., Kurfess J. D., eds, AIP Conf. Proc. 410, Proc. 4th Compton Symposium. Williamsburg, VA

This paper has been typeset from a TEX/LATEX file prepared by the author.